Three-Dimensional Structure in Water−Methanol Mixtures

A. Laaksonen*,†

Division of Physical Chemistry, Arrhenius Laboratory, Stockholm University, S-106 91 Stockholm, Sweden

P. G. Kusalik‡ and I. M. Svishchev§

Department of Chemistry, Dalhousie University, Halifax, Nova Scotia, Canada B3H 4J3

Received: February 24, 1997; In Final Form: June 2, 1997⊗

The diverse properties of hydrogen-bonded liquids and solutions must manifest their unique local structures. An unambiguous three-dimensional picture of the local ordering in these liquid systems is not accessible through radial distribution functions, the usual outputs of computer simulation, or experimental studies. In this work we employ spatial distribution functions to analyze the three-dimensional local structure in water−methanol solutions. Molecular dynamics simulations are performed at room temperature for five water−methanol liquid mixtures scanning the entire range of compositions. The effects of the alcohol on water structure and water on methanol structure are considered in detail. The results are compared to previous simulations and discussed from the point of view of various solvation models. Large structural changes are observed, many of which are not apparent from simple radial analysis. In water-rich solution we confirm a high degree of ordering, characterized by a very strong preference for tetrahedral arrangements, where the water molecules appear most highly localized around the hydroxyl group of the methanol solute. Strongly hydrated methanol molecules adopt rather specific relative positions that most readily accommodate the ordering within their hydration cages. In methanol-rich solution the local structure very closely resembles that of pure methanol. We find that rather long equilibration periods appear to be necessary to obtain accurate structural information in computer simulations of these complex systems.

1. Introduction

There are numerous ways to categorize solvents, for example, according to their physical chemical properties, their acidity/basicity, or their specific interactions with various solutes.[1] However, there exists no unique way to do a general classification, depending on characteristic differences between, on one hand, organic and inorganic solvents, or on the other, between water and non-aqueous solvents. As a solvent,[2] water occupies a unique position due to its abundance on Earth and its key role in biological systems. None of the nonaqueous solvents possess all the remarkable solvent and ionizing properties exhibited by water, yet water almost completely lacks[3,4] the ability to solvate nonpolar molecules.

One possible way to classify solvents would be according to their three-dimensional liquid structure. Water is known to be a highly structured liquid. Although the structure in liquid water has been the subject of considerable scientific debate, one accepted but somewhat simplified picture consists of a hydrogen-bonded tetrahedrally coordinated network similar to ice where some of the interstitial cavities are filled by water molecules.[5] This local tetrahedral structure of water exists for only a limited time (perhaps less than 0.1 ps) and is continuously changing through the breaking and formation of hydrogen bonds. A varied assortment of other pictures have been used to describe the structure in water, including a mixture of different types of regions from free water to random bound and ordered regions, chains, and small polymers, cages, and holes.[1]

Alcohols, such as methanol, are also structured, associated liquids. Instead of forming tetrahedral networks, alcohols appear to prefer to form winding polymeric chains;[1] these chain structures are characteristic[6] of their solid state. On the basis of computer simulation results, the associated molecules within the hydrogen-bonded chains in alcohols have been found to have appreciably (an order of a magnitude) longer lifetimes compared to neighboring water molecules within its three-dimensional networks.

Water and alcohols, both, are complicated liquids and a challenge to study theoretically. Naturally, mixing them results in a far more complex liquid system.[7−9] If a small amount of alcohol (or another polar organic molecule, such as acetone, dimethyl sulfoxide, or tetrahydrofuran) is added to water, the water structure is believed to become enhanced in a way similar to that found when a nonpolar solute is dissolved in water. This phenomenon was first discussed by Frank and Evans.[10] Mixed solvents in general, of which a water−alcohol mixture is an example, show many unusual properties, often quite different from those observed for the pure components of the mixture.[1] In some cases, certain substances are not soluble in the pure components, while they may be readily soluble in the solvent mixtures and *vice versa*. Binary mixtures are frequently used as solvents in chemistry, and aqueous mixtures in particular are important in many industrial applications because of the remarkable flexibility some of these mixtures offer as solvents.[7] An interesting phenomenon, related to mixed solvents, is selective or preferential solvation of salts in mixed solvents in which the ions may concurrently be solvated by the pure components in the mixture.[11]

Methanol, the simplest (smallest) alcohol, is a suitable model molecule for studies of several structural aspects of solvation in aqueous mixtures. The methyl group is assumed to reinforce the water structure, at least in diluted aqueous solutions, while the hydroxyl group makes the whole molecule soluble in water. It was suggested earlier that methanols in diluted aqueous

† E-mail: aatto@tom.fos.su.se.
‡ E-mail: kusalik@is.dal.ca.
§ E-mail: sigor@is.dal.ca.
⊗ Abstract published in *Advance ACS Abstracts,* July 15, 1997.

S1089-5639(97)00673-7 CCC: $14.00

solutions would simply substitute waters in the hydrogen-bonded water structure. Now, the neutron diffraction studies by Soper and Finney[12] suggest, in accordance with most of the previous computer simulation studies, that there exists a shell of water molecules, forming a distorted cage, around the methanol molecule. This cage around the methyl group is believed to consist of roughly 20 water molecules and is thought to be comparable to the water clathrate around a methane molecule.

The water−methanol mixtures studied in this work span the entire concentration range; the five methanol mole fractions, X_m, examined in our computer simulations are 0.062, 0.25, 0.5, 0.75, and 0.938. Our main objective is to analyze the solvation structure in detail using a new tool, spatial distribution functions (SDF). The SDF approach, originally developed by Svishchev and Kusalik for the study of liquid water structure,[13,14] has been further employed to examine pure methanol.[15] The present work is therefore a natural continuation in this series, which hopes to provide a more detailed understanding of the microscopic structure of molecular liquids and solutions.

Several computer simulation studies of aqueous methanol solutions have been previously reported in the literature. Okazaki et al.,[16] Bolis et al.,[17] and Jorgensen and Madura[18] published the first computer simulation studies of methanol dissolved in water. The methyl rotation was allowed in the model used by Jorgensen and Madura. In spite of different models and some contradictions in their results, they all found a cagelike structure around the methyl group. Later, Stouten and Kroon[19] confirmed the well-known volume contraction in the mixing of water and methanol in their MD simulation using the SPC water model[20] and a three-site single-point model for methanol[21] (with a Me−O−H bending allowed). These effective potential models, which have been optimized for the pure components, were used without any corrections in an equimolar mixture of water and methanol. Ferrario et al.[22] report an extensive study of aqueous solutions, including methanol, for the concentrations X_m of 0.125, 0.25, 0.50, 0.75, and 0.875, and Palinkas et al.[23−25] report a series of investigations with methanol mole fractions of 0.1, 0.25, and 0.9; both sets of studies employed effective potential models. Tanaka et al.[26,27] have shown that the water−water interactions can play an important role in determining some of the properties of water−methanol solutions.

2. Computational Details

The water model used in our study is the three-site single-point-charge (SPC) potential,[20] while for methanol we have used the model of Haughney et al.,[28] which is a three-site model where the methyl group is described by a single site. Both molecular models are treated as rigid. The model potentials contain terms that account for the interactions between Lennard-Jones spheres and fractional charges, assigned to represent the (permanent) molecular charge distributions, associated with each site. Further details of the potential parameters can be found in the original papers[20,28] and are not repeated here.

All simulations were carried out in the NVT ensemble, using a cubic simulation cell furnished with periodic boundary conditions. The equations of motions were solved with a time step of 1 fs. The translational equations of motion were integrated using the Verlet leap frog algorithm[29] and the rotational motion using the quaternion-based leap frog method by Fincham.[30] The cutoff distance for the Lennard-Jones interactions was set equal to half of the box length, based on the center-of-mass of the molecules. The long-ranged Coulombic interactions were treated using the Ewald summation technique[29,31] rather than using shifted cutoff or switching function techniques, which have been shown[32] to have significant impact on the simulation results. The simulations were carried with a modified version of McMoldyn[33] on the departmental IBM 6000/590 workstation at the division of Physical Chemistry, Stockholm University, and on the Alliant FX 2800/16 formerly at Dalhousie University.

TABLE 1: Simulated Water−Methanol Solutions

	run				
	I	II	III	IV	V
number of H_2O	240	192	128	64	16
number of MeOH	16	64	128	192	240
X_m	0.062	025	0.5	0.75	0.938
ρ (g/cm^3)	0.97	0.93	0.885	0.84	0.80
T (K)	300	300	300	300	300
timestep (fs)	1.0	1.0	1.0	1.0	1.0
duration (ps)	200	200	200	200	200

TABLE 2: Coulombic and Lennard-Jones Contributions to the Total Interaction Energies, U_{tot}/N_{tot}: WW = Water−Water, WM = Water−Methanol, MM = Methanol−Methanol; All Energies Are in kJ/mol; See Table 1 for More Details

run	contribution	Coulomb	Lennard-Jones
I	WW	−49.8	10.4
	WM	−5.52	0.09
	MM	0.02	−0.10
II	WW	−34.3	6.72
	WM	−14.9	0.52
	MM	−2.04	−0.91
III	WW	−16.0	3.22
	WM	−22.2	1.57
	MM	−5.64	−2.59
IV	WW	−4.29	0.81
	WM	−17.3	1.96
	MM	−15.2	−3.99
V	WW	−0.43	0.09
	WM	−5.59	0.54
	MM	−25.4	−5.32

3. Simulated Systems

Five different water−methanol solutions were prepared in this computational study: two diluted and two concentrated with respect to each of the components as well as an equimolar mixture. Some physical parameters and simulation data are given in Table 1. These five mixtures were chosen to represent the various typical cases along the concentration axis for the binary mixture of water and methanol.

Prior to our production runs, each of the mixtures is equilibrated for more than 0.5 ns. During these long equilibration runs, rather slow relaxations of the local structure were observed as changes (not attributable to numerical noise) occurring in the measured $g(r)$ over periods of tens of thousands of time steps. It was also noted that the details of the local structure (as seen in the SDFs) appeared rather sensitive to the temperature in the simulation.

Results for various dynamical properties and many other typical quantities obtained in MD simulations will not be explicitly reported here; we will note simply that our results coincide with those reported in previous studies.[22−27]

4. Interaction Energies

The average potential energies can be divided into short-range (Lennard-Jones) and long-range (Coulombic) contributions to investigate the significance of specific interactions to changes in the local structure. Averages for these potential energy contributions are given in Table 2 for each of the five runs (without normalizing them with respect to the mole fractions). The energies quoted do not include the long-range corrections to the Lennard-Jones interactions as well as the self-term to the

TABLE 3: Water, Methanol, and Total Interaction Energies (in kJ/mol)

run	water−water $\langle U_{ww}/N_w \rangle$	methanol−methanol $\langle U_{mm}/N_m \rangle$	total $\langle U_{tot}/N_{tot} \rangle$
I	−42.0	−1.2	−44.9
II	−36.8	−11.8	−44.9
III	−25.5	−16.5	−41.6
IV	−13.9	−25.6	−38.0
V	−5.4	−32.8	−36.1

Ewald reciprocal-space energy (which cannot be divided between the different component pairs). These two corrections are very small (typically on the order of our uncertainties, roughly 1% of the total) and opposite in sign; thus they effectively cancel. Interestingly, the Coulombic contribution is attractive for all the runs and species pairs (see Table 2), except for MM in run I, for which it is vanishingly small. The Lennard-Jones contribution is consistently repulsive for water−water and water−methanol pairs, while it is attractive for all methanol−methanol interactions.

For the sake of comparison, it is also useful to examine the water−water, methanol−methanol contributions to the total average energies normalized per molecule of that species (i.e., before multiplication by the respective mole fraction) as well as the total average interaction energy. These are shown in Table 3 for all five concentrations. We find that the water−water energy for the water-rich solution, −42.0 kJ per mol of water, is close to the value obtained for pure SPC water, −41.4 kJ/mol. This suggests a slight increase in the water−water correlations for this dilute solution. As the methanol content is further increased, the corresponding water−water energies begin to increase (decrease in magnitude), first slowly (from $X_m = 0.062$ to 0.25), after which they increase more rapidly and monotonously, reflecting the simple fact that any particular water molecule is surrounded by fewer water molecules. Starting from pure methanol, we see that the methanol energies increase monotonously, with the methanol−methanol energy at $X_m = 0.938$ already being well above the corresponding value for pure methanol at room temperature, as the methanol content of the solution is reduced. Clearly, the methanol−methanol and water−water energies suggest different structural changes upon initial dilution.

The cross-interaction contribution to the total energy is largest in magnitude for the equimolar mixture, indicating strong attractive interactions between unlike molecules. As a result, we would expect water and methanol to mix well. However, the strength of the unlike-pair interaction, for which simple Lorentz−Berthelot combination rules have been used, has likely been overestimated. It is known[34] that these combination rules give an exaggerated potential well depth for cross-interaction terms.

5. Solution Structure from Radial Distribution Functions

The structure within water−methanol mixtures at several different concentrations has been examined already at the radial distribution function (RDF) level by previous workers.[22−28] However, as shown by Svishchev and Kusalik,[13−15] much of the detailed information of the local liquid structure can be lost in a radial analysis. Averaging over the angular coordinates of the pair distribution functions can often result in the cancellation of contributions from regions of low and high probability at the same distance but composing different parts of the local structure in solution. Strictly speaking, radial distribution functions provide a complete structural picture only for liquids of spherical particles. Structural analyses of aqueous systems going beyond radial averages have been previously attempted,[35] and together with the work of Svishchev and Kusalik,[13−15] indicate that for strongly associating molecules, like water or molecules with hydrophilic and hydrophobic parts as methanol, much of the detail of the local structure is lost in simple (one-dimensional) radial analysis. To demonstrate this point, we have shown our radial distribution functions between the various pairs of oxygen atoms in Figure 1. The heights of the first maxima in the $g_{OO}(r)$ are compared in Figure 2. We have also calculated coordination numbers for both water and methanol molecules by integrating the appropriate RDFs to their first minima; the results are presented in Figure 3. For the sake of data management and ease of comparison, we have chosen to focus exclusively on oxygen−oxygen correlations in this study. While further analysis with the hydrogens and carbon included may provide further detail, we do not believe they would add to the qualitative picture outlined below.

Focusing first on water−water correlations, we see from Figures 1a and 2 that the first maximum in $g_{OO}(r)$ increases monotonously with methanol concentration. An interpretation of this behavior is the enhancement of the water structure due to the presence of the methanol, as proposed by Frank and Evans.[10] Certainly, in a water-rich mixture ($X_m = 0.062$) we also see a strong enhancement of the secondary (tetrahedral) structure relative to that found for pure SPC water. Yet for higher methanol compositions ($X_m \geq 0.5$) we find that beyond its first peak $g_{OO}(r)$ appears rather featureless, which could be interpreted as indicating a lack of secondary correlations. We see from Figure 1a that the water oxygen−oxygen nearest-neighbor distance is essentially independent of the methanol content for these systems.

The large first maxima in the water−water $g_{OO}(r)$ for our methanol-rich solutions suggest that there is a rather high degree of association of water molecules (as dimers, etc.) in these systems. This supposition is supported by the relatively large water−water interaction energies given in Table 3 and by the water coordination number around water, roughly 0.4, for $X_m = 0.938$. Inspection of several configurations of this system does reveal that roughly half the water molecules are paired. Comparison with previous work[22−25] reveals similar trends in the first maxima. The results of Palinkas et al.[23−25] show the same trend, although less marked, while the peak heights reported by Ferrario et al.[22] clearly decrease above $X_m = 0.6$. Whether this apparent disagreement with the latter behavior is due to inadequate sampling in these previous calculations (we have already discussed an apparent slow convergence in the structural functions for these mixed systems) or is due to differences in potential models is unclear. Previous workers[16,26,27] have observed other sensitivities to the choice of interaction potentials, emphasizing the difficulties that are likely to arise in trying to describe a complex system like a water−methanol mixture using simple empirical potentials together with simple combining rules.

The first maxima in the methanol−methanol RDF, $g_{OO}(r)$, decrease with decreasing methanol concentration, as can be seen from Figures 1b and 2. This suggests that the methanol−methanol structure (in contrast to water) is gradually lost as this component becomes more dilute. Such a picture might appear reasonable since it would be hard to imagine the simultaneous enhancement of both the liquid water and liquid methanol structures. For the lowest concentration studied, $X_m = 0.062$, the first peak in $g_{OO}(r)$ has all but disappeared, with the entire function appearing rather featureless. One could conclude that the methanol molecules have essentially become completely hydrated and that methanol−methanol correlations have become almost nonexistent. These observations are consistent with the earlier work of Ferrario et al.[22] and Palinkas et al.[23−25]

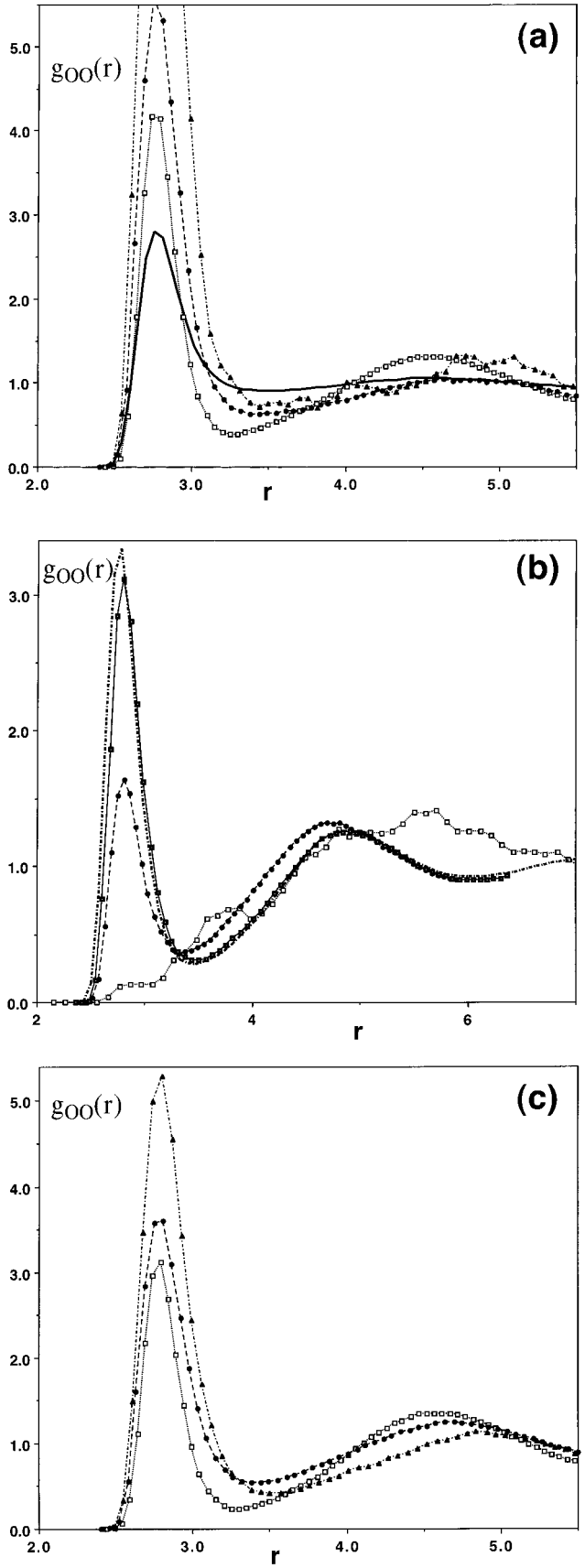

Figure 1. Radial distribution function, $g_{OO}(r)$, for oxygen atoms in various water−methanol solutions. The open squares, dots, and triangles represent results of solutions with $X_m = 0.062$, 0.5, and 0.938, respectively, while the solid and dashed lines are data from pure water and pure methanol, respectively: (a) water−water; (b) methanol−methanol; (c) water−methanol.

Curves for $g_{OO}(r)$ for water−methanol pairs are shown in Figure 1c. We find that the first peaks become higher (see Figure 2) and that these RDFs generally become more structured as the methanol content of these solutions is increased. This is perhaps surprising since one might intuitively expect the largest peak heights for the equimolar solution where the number of possible cross-correlations is maximized. It is also apparent from Figure 1c that the position of the second maximum shifts to slightly larger separations with increasing X_m. Again, our results are in agreement with those of previous workers.[22−25]

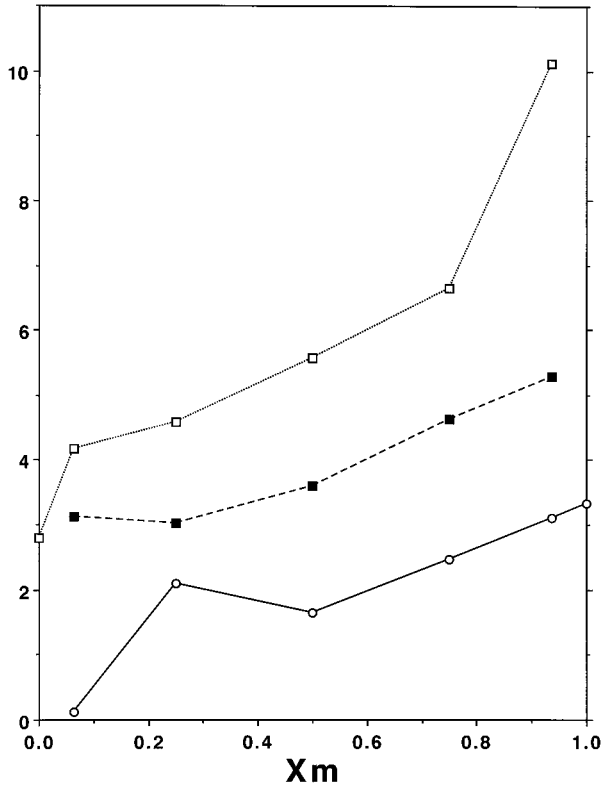

Figure 2. Composition dependence in the $g_{OO}(r)$ peak heights. The open squares, solid squares, and open circles are the observed maxima for the water−water, water−methanol, and methanol−methanol functions, respectively. The value recorded for the methanol−methanol function at $X_m = 0.062$ was taken at a separation of 2.8 Å.

Several features in the estimated coordination numbers (around oxygen atoms) can be seen in Figure 3. We note that these coordination numbers are around oxygen atoms and hence the nearest neighbors detected are probably hydrogen (H-) bonded to the central molecule. The "structure-making" in water with the initial addition of methanol is evident, as the total coordination around a water molecule drops from about 4.5 in pure water to 4.0 in the water-rich mixtures. In general, we see in Figure 3 that water has higher coordination numbers (total or species specific) than methanol; the total coordination around a water is consistently about one molecule larger than for methanol, over the entire composition range. For water in methanol-rich solutions and for methanol in water-rich mixtures, their total coordination numbers approach 3. This behavior can be explained by noting that water is a double H-bond donor, whereas methanol can be a donor of only a single H-bond (both can be double acceptors). Thus, as pure liquid, water prefers four H-bonded neighbors (two donors, two acceptors), while methanol has only two (single donor, single acceptor). In concentrated mixtures, the "solutes" appear to take on some of the H-bond character of the "solvent" (e.g., water in methanol-rich solutions tending to be a single H-bond acceptor, or methanol in water-rich solutions tending to be a double H-bond acceptor). Certainly we would expect a competition for H-bonds in any mixture of these two liquids (since there are more acceptor than

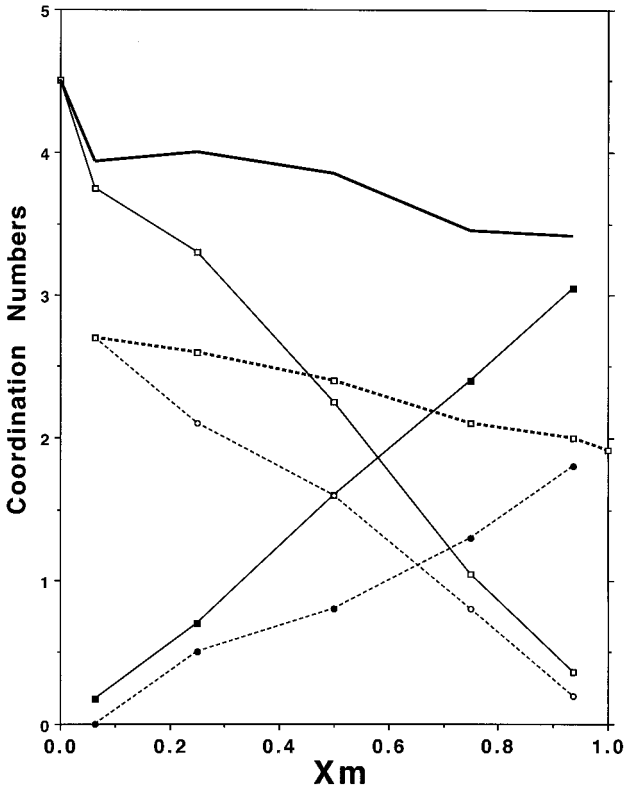

Figure 3. Composition dependence of the various coordination numbers for water and methanol molecules in their binary mixtures. The heavy solid and heavy dashed lines are the total (water plus methanol) coordination numbers for water and methanol molecules, respectively. The open squares and solid squares, respectively, are values for the average numbers of water and methanol molecules found near a given water molecule, while the open circles and dots, respectively, represent the numbers of water and methanol molecules observed around a given methanol molecule.

donor sites), and the balance that is finally achieved must be critically important in determining the properties of the solution. This explanation is supported by specific results in the spatial distribution function analysis given below.

6. Solution Structure from Spatial Distribution Functions

The spatial distribution functions between all independent atomic pairs would completely describe the three-dimensional neighborhood surrounding a given molecule (which defines the local frame). A spatial distribution function is straightforward to calculate from a multidimensional array that is a simple generalization of a standard RDF accumulator. Rotation matrices must first be constructed for all the molecules at each time step to allow the rotation of all distance vectors into the local molecular coordinate system. This can be easily done, as in the present case, if the molecular orientations are described in terms of quaternions. In the case of flexible molecules where the rotational motion is not treated explicitly, the rotation matrix can be constructed using the eigenvectors after the diagonalization of the moment of inertia tensor for each molecule at each time step; the computing time required is comparable to that of the SHAKE procedure.[36,37]

An analysis based on spatial distribution functions does require that large amounts of data first be collected and then visualized. The presentation of these three-dimensional functions also poses special difficulties. In this study we find that the oxygen−oxygen functions, $g_{OO}(r,\Omega)$, are sufficient to provide us a detailed picture of the structure in solution. As in previous work with water[13,14] and methanol,[15] $\Omega \equiv \{\theta,\phi\}$ represents the angular coordinates of the separation vector,

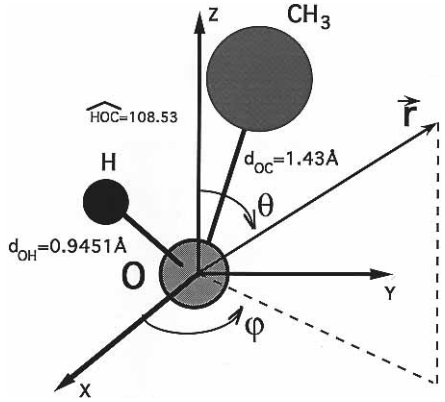

Figure 4. Definition of the local frame of a methanol molecule. Note that the plane of the molecule lies in the *XZ*-plane.

where θ is the angle between the separation vector r and the local z-axis, and ϕ is its angle away from the planes of the respective molecules. For water the local z-axis is defined to be along its dipole moment, while for methanol the z-axis is the bisector of the COH angle (see Figure 4).

Figure 5 demonstrates some of the compositional dependence in the water−water SDFs, where the r,θ dependence in $g_{OO}(r,\Omega)$ is displayed for $\phi = 90$ (i.e., perpendicular to the plane of the molecule). The compositional dependence for the peaks observed in the SDFs is shown in Figure 6 for both H-bond-donating ($\theta > 90°$) and H-bond-accepting ($\theta < 90°$) neighbors. In Figures 7, 8, 9, and 10 we present three-dimensional isosurface representations of the $g_{OO}(r,\Omega)$ between water−water, water−methanol, methanol−water, and methanol−methanol, respectively, at various compositions. We note that in spatial analysis, the water−methanol and methanol−water functions are unique. In the discussion that follows we will adopt the convention that the first label will identify the central molecule while the second indicates the surrounding species.

It is clear from Figure 5 that the addition of a small amount of methanol to pure water significantly perturbs the water−water structure. In particular, we see in Figure 5b that the peak due to nearest H-bond-donating neighbors becomes much sharper and localized to its ideal tetrahedral position, the secondary structure generally becomes more pronounced, and the feature attributed to nontetrahedral (interstitial) coordination in pure water (see Figure 5a) has essentially disappeared. These structural changes are all consistent with the notion of "structure-making" in this water-rich solution. In methanol-rich solution, as in Figure 5c, we find that the water−water structure has lost most of its tetrahedral character. We see that the peak due to H-bond-donating neighbors is now a single feature in a dipolar (i.e., $\theta = 180°$) position. A secondary dipolar feature has also become prominent for θ near 0° and for separations around 3.5 Å.

To help compare the nature of the local structure around water and methanol in these mixtures, we have plotted in Figure 6 the composition dependences of the peak heights in $g_{OO}(r,\Omega)$ for H-bond-accepting and H-bond-donating neighbors. The distinction between H-bond-accepting and -donating neighbors is important, as we can see that the ordering of the peak heights is different in each case for all but one solution. If we interpret these peak heights as measures of relative preference for H-bonding in solution, then several observations can be made. Both water and methanol prefer to have a water molecule as a H-bond-accepting or -donating neighbor. From Figure 6a we see that the peaks due to both water and methanol H-bond-accepting neighbors are generally larger around water than around methanol. In Figure 6b we find that the peaks for methanol acting as a H-bond-donating

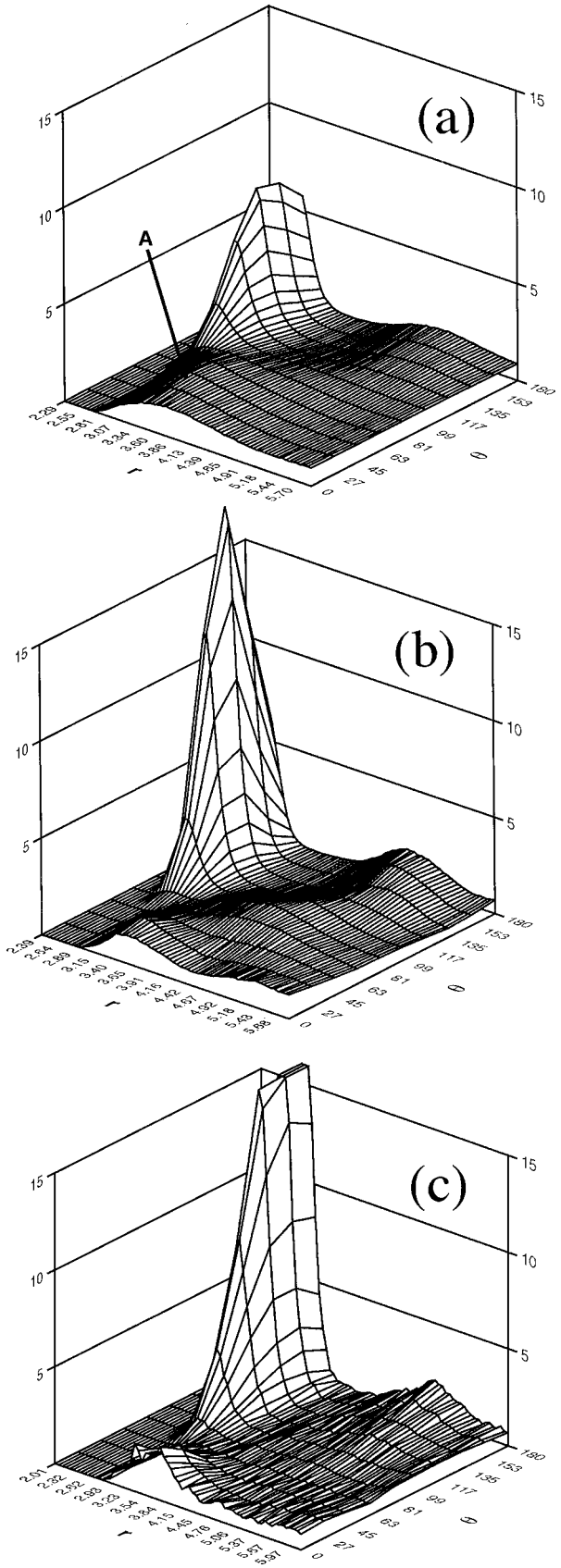

Figure 5. Composition dependence in the water−water spatial distribution function, $g_{OO}(r,\Omega)$. The "slice" of the function perpendicular to the plane of the molecule (i.e., $\phi = 90°$) is shown: (a) the result for pure SPC water, (b) from a solution with $X_m = 0.062$, and (c) for a mixture where $X_m = 0.75$. In part a A indicates the feature due to additional nontetrahedral coordination. The peak in part c has been truncated, its true maximum approaching $\theta = 180°$ being 23.4.

neighbor are roughly half the height of those for water, as we might expect. We also observe a strong asymmetry for unlike

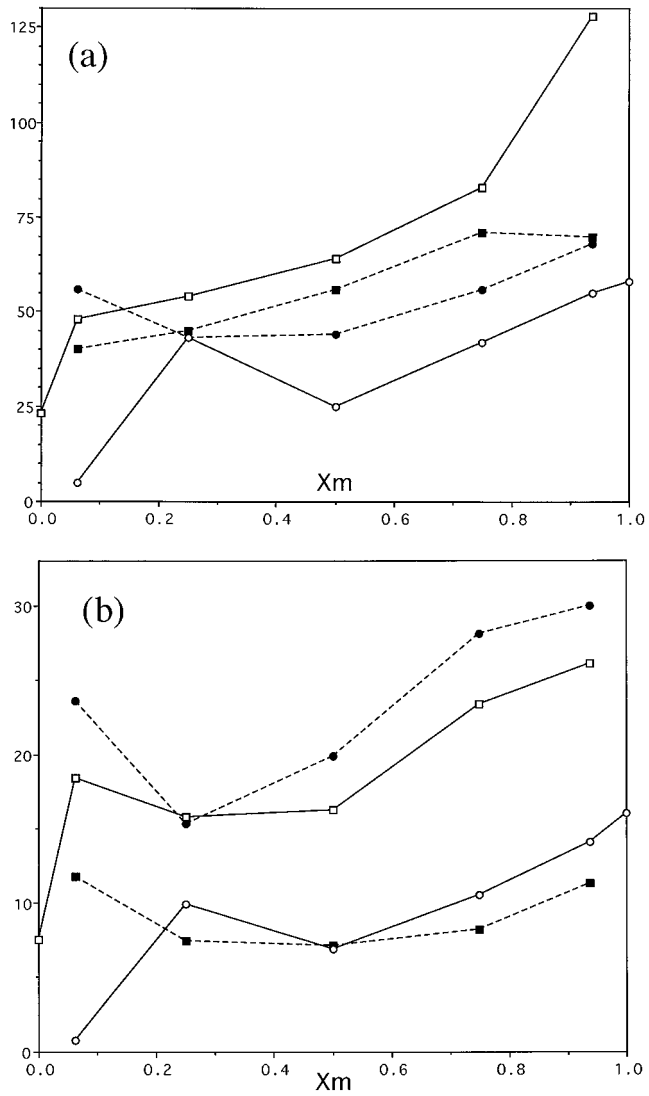

Figure 6. Composition dependence in the $g_{OO}(r,\Omega)$ peak heights. The open and solid squares, respectively, represent values for water and methanol around a water molecule, while the dots and open circles are results for water and methanol, respectively, around a methanol molecule: (a) peak heights for H-bond-accepting ($\theta < 90°$) neighbors and (b) peak heights for H-bond-donating ($\theta > 90°$) neighbors.

pairs, because while methanol generally appears as the weakest H-bond donor for water, water is the strongest H-bond donor for methanol.

The composition dependence apparent in Figure 6 might seem to suggest that these solutions generally become more structured as the methanol content is increased; both the H-bond donor and H-bond acceptor peaks increase with increasing X_m, although some important deviations from this behavior are evident for water-rich solutions. Yet such an interpretation must be regarded with care, for as we have already noted, for example, as X_m increases, the pair of (tetrahedral) peaks due to H-bond-donating neighbors become a single (dipolar) peak.

Perhaps the most complete understanding of the local structure in these systems can be obtained from the examination of isosurfaces of $g_{OO}(r,\Omega)$ displayed as three-dimensional maps. Shown in Figure 7 are density maps for the water−water structure for two different water−methanol solutions. We note that specific water−water results for $g_{OO}(r,\Omega)$ have already been discussed in Figure 5 for the particular case of $\phi = 90°$. Examination of Figure 7a, for an equimolar solution, reveals the usual features due to nearest H-bonded neighbors (the two caps over the hydrogens and the cupped feature below the molecule) found in pure water.[13,14] These features remain

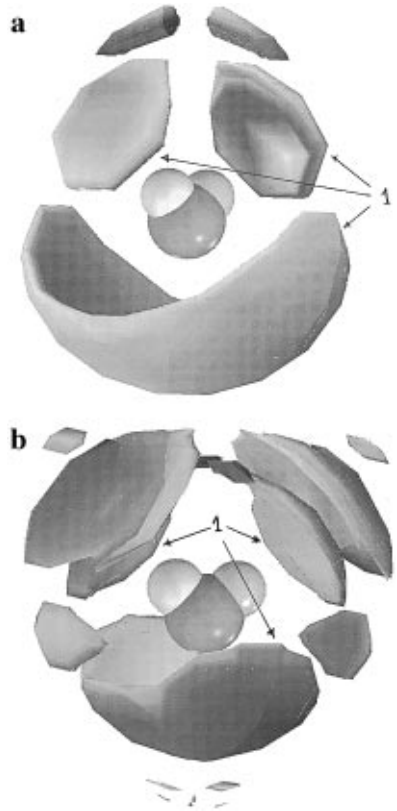

Figure 7. Water−water spatial distribution functions, $g_{OO}(r,\Omega)$, for water−methanol solutions with (a) $X_m = 0.5$ and (b) $X_m = 0.938$. In part a the isosurface $g_{OO}(r,\Omega) = 2.0$ is shown, while in part b the surfaces visualized correspond to $g_{OO}(r,\Omega) = 2.25$. The central molecule has been included to define the local frame. 1 indicates features due to nearest neighbors.

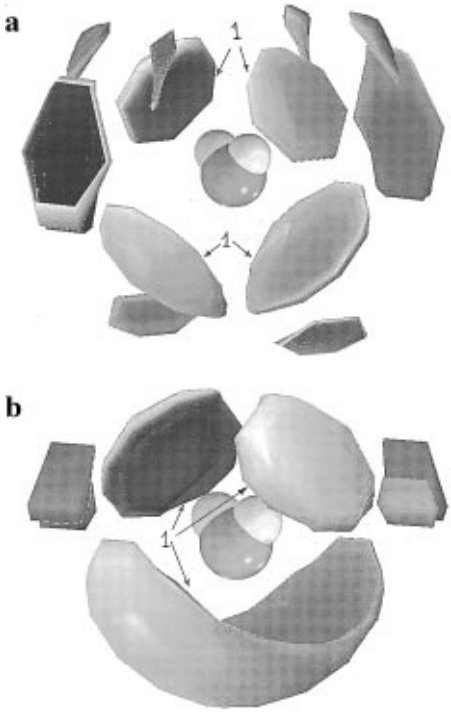

Figure 8. Water−methanol spatial distribution functions, $g_{OO}(r,\Omega)$, for water−methanol solutions with (a) $X_m = 0.062$ and (b) $X_m = 0.938$. In part a the surfaces correspond to $g_{OO}(r,\Omega) = 2.0$, while in part b the isosurface threshold is 1.65. The central molecule has been included to define the local frame. 1 indicates features due to nearest neighbors.

almost unchanged over the entire composition range, perhaps the most significant change being a narrowing of the waist of the H-bond donor feature as the methanol content is reduced,

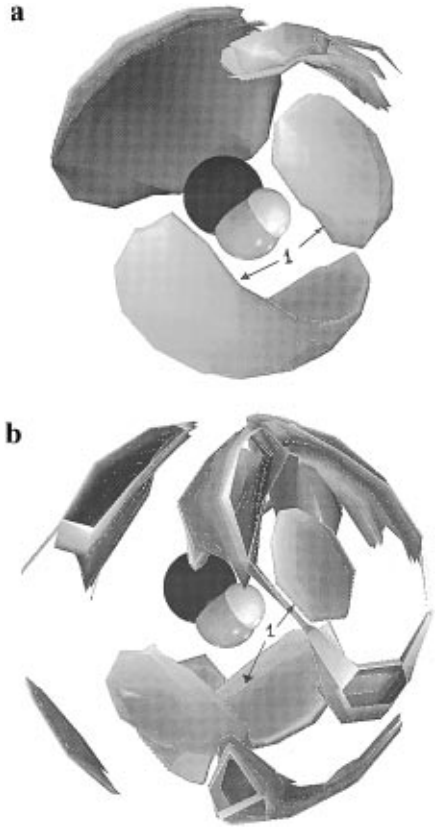

Figure 9. Methanol−water spatial distribution functions, $g_{OO}(r,\Omega)$, for water−methanol solutions with (a) $X_m = 0.938$ and (b) $X_m = 0.062$. In both parts a and b the surfaces shown correspond to an isosurface threshold of 1.8. The central molecule has been included to define the local frame. 1 indicates features due to nearest neighbors.

indicating greater tetrahedral character. Missing from Figure 7a, and all similar maps for all the water−methanol solutions examined, are the two "interstitial" features due to nontetrahedral near neighbors which are important in the characterization of the local structure in pure water.[13,14] Rather, in Figure 7a we see a dipolar ($\theta \approx 0°$) feature not found in pure water corresponding to separations of about 3.5 Å, as was noted in Figure 5. We point out that the apparent splitting of this feature in Figure 7a is an artifact of the pole singularity in our spherical polar representation of the data. This dipolar feature is found in all the mixed systems studied, but is most prominent in the equimolar mixture, and arises from two water molecules near a common methyl group.

Figure 7b shows the water−water structure in a methanol-rich solution. It can be easily seen that there is considerable structure in the water−water spatial correlations extending out to large separations (due, for example, to two water molecules sharing a common H-bonded methanol neighbor). This observation is in sharp contrast to the behavior evident in Figure 1a, where the angle-averaged function $g_{OO}(r)$ shows almost no evidence of secondary structure for this solution.

The spatial structure of methanol around water is shown in Figure 8 for water-rich and methanol-rich solutions. In Figure 8a four well-defined features due to nearest H-bonded neighbors indicate the strong tetrahedral character of the local structure in this water-rich mixture. Several smaller features, attributable to the second neighbor structure, are also evident in Figure 8a, but the remaining two large features in equatorial positions correspond to a methanol nearest neighbor with the methyl group pointing toward the water molecule (or equivalently the central water molecule lying near and perpendicular to the methyl group of a methanol molecule). This feature has a maximum at a separation of about 4.5 Å and appears over the entire composi-

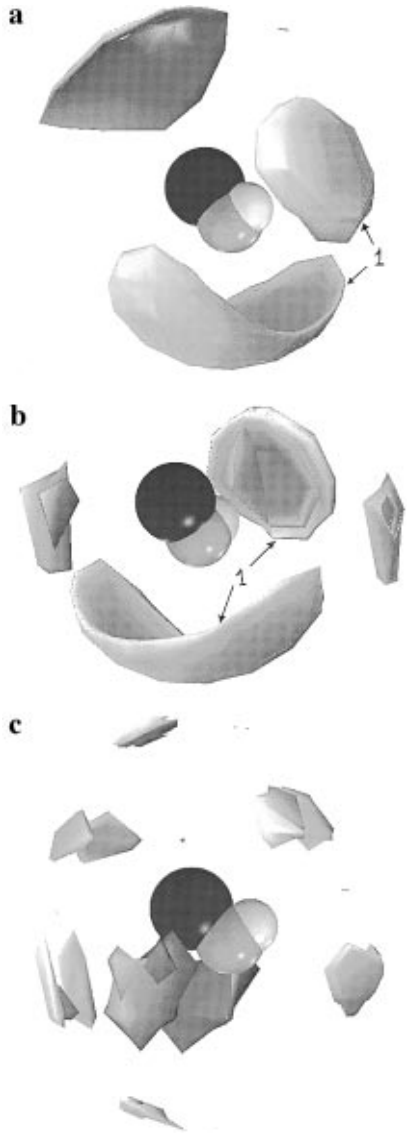

Figure 10. Methanol−methanol spatial distribution functions, $g_{OO}(r,\Omega)$, for water−methanol solutions with (a) $X_m = 0.938$, (b) $X_m = 0.5$, and (c) $X_m = 0.062$. In parts a and b the isosurfaces $g_{OO}(r,\Omega) = 1.75$ are shown, while in part c the surfaces visualized correspond to neighboring methanol−oxygen density 4.5 times that found in the bulk solution. The central molecule has been included to define the local frame. 1 indicates features due to nearest neighbors.

tion range (see Figure 8b). For a methanol-rich solution, as in Figure 8b, the SDF appears less structured. A single cupped feature can again be seen below the central water molecule, which can be shown (with more detailed analysis) to contain only a single maximum at $\theta = 180°$.

In Figure 9 we have shown three-dimensional isosurface representations of $g_{OO}(r,\Omega)$ for methanol−water at two different compositions. The water structure around methanol in methanol-rich solution is very similar to that found for methanol−methanol in the same mixture, as can be seen by comparing Figure 9a with Figure 10a. The strong tetrahedral character of the local structure in the water-rich solution is clearly evident in Figure 9b, where a splitting of the nearest H-bond donor feature and distinct second-neighbor coordination in tetrahedral positions can be seen. Moreover, we find that the apparent focal point of the strong tetrahedral ordering of the water around the methanol is *not* the methyl group, but rather the hydroxyl group. A more careful examination of $g_{OO}(r,\Omega)$ adjacent to the methyl group reveals, in fact, little specific structuring of the water (relative to this site). This result is consistent with the recent work of Liu and Brady[38] that examines in considerable detail the water structure around sugar (pentose) molecules in aqueous solution using a SDF approach. They also observe strong local ordering around hydroxyl groups and "weak localization effects" near hydrophobic regions. We would suggest that structural analysis, such as that attempted by Soper and Finney,[12] might more profitably focus on the hydroxyl rather than the methyl group of the methanol.

The composition dependence in the three-dimensional methanol−methanol structure is explored in Figure 10. In methanol-rich solution we find that the local structure very closely resembles that found in pure methanol (note that Figure 5 of ref 15 displays a lower isosurface threshold value); features due to a single H-bond-donating and a single H-bond-accepting neighbor as well as a board cap over the methyl group attributed to interchain neighbors are apparent. In the equimolar mixture, there is a general reduction in the local structure as manifested in Figure 10b with the disappearance of the cap over the methyl group. We would predict from the methanol−oxygen methanol−oxygen *radial* distribution function (see Figure 1b) that in water-rich solution methanol is essentially completely hydrated, but otherwise there is little correlation between methanol molecules. Yet, it can be clearly seem from the full spatial map displayed in Figure 10c that this is *not* the case. Whereas it is true that the nearest H-bond coordination has disappeared, an array of specific secondary coordination features is now apparent; we should also point out that the density threshold used in Figure 10c is 4.5 times that of the bulk. This rich secondary structure would imply that the strongly hydrated methanol molecules adopt quite specific relative (spatial) positions that most readily accommodate the ordering within their hydration cages.

7. Conclusions

In this study, molecular dynamics simulations are performed at room temperature for water−methanol liquid mixtures with compositions (methanol mole fractions) of $X_m = 0.062$, 0.25, 0.5, 0.75, and 0.938. The local structure in solution has been investigated in detail, our analysis being principally based on oxygen−oxygen spatial distribution functions. In our simulations, equilibration periods of 0.5 ns appeared to be necessary to allow for slow relaxations evident in the local structure.

We have demonstrated that radial distribution functions provide an incomplete and sometimes misleading picture of the local order in these liquid mixtures. We find that the local structure in these mixed systems and its composition dependence are rather complex. The basic underlying structural patterns appear to be largely determined by that preferred by the dominant species in these binary mixtures; in particular we observe that the number of nearest neighbors for both water and methanol decrease by one in going from water-rich to methanol-rich solutions. The competition for H-bond sites can be seen to play an important role in affecting the nature of the short-range order around molecules of both species.

In methanol-rich solution the water−water correlations are very pronounced even at longer range, while methanol retains most of its pure liquid structure. In water-rich solution we observe a strong accentuation of the tetrahedral character in the local structure. "Structure-making", the enhancement of the tetrahedral order in the water−water structure over that found in the pure liquid, is clearly evident. Yet, the ordering of water molecules around the methanol solutes is perhaps even more dramatic. Moreover, we find that the water structure around a methanol molecule is much more localized around the hydroxyl rather than the methyl group. Very distinctive methanol−methanol correlations are evident at longer range, consistent with the suggestion that each methanol is strongly solvated by a "cage" of water molecules.

The results presented in this study are consistent with existing experimental data for water−methanol systems obtained from neutron scattering[12] and from light scattering.[39] The new structural insights provided should aid both in the interpretation of existing experimental results and in suggesting further experimental work.

Acknowledgment. This work has been supported by the Swedish Natural Science Research Foundation, NFR (A.L.), and by the Natural Science and Engineering Research Council of Canada, NSERC (P.G.K.).

References and Notes

(1) Reichardt, C. *Solvents and Solvent Effects in Organic Chemistry*, second revised and enlarged edition; VCH: Weinheim, 1988.

(2) Eisenberg, D.; Kauzmann, W. *The Structure and Properties of Water*; Oxford Academic Press: New York, 1969.

(3) Tanford, C. *The Hydrophobic Effect: Formation of Micelles and Biological Membranes*; Wiley: New York, 1973.

(4) Israelachvili, J. *Intermolecular and Surface Forces*, 2nd ed.; Academic Press: New York, 1991.

(5) Popovych, O.; Tomkins, R. P. T. *Nonaqueous Solution Chemistry*; J. Wiley: New York, 1981.

(6) Hamilton, W. C.; Ibers, J. A. *Hydrogen Bonding in Solids*; Benjamin: New York, 1968.

(7) Franks, F. *Water−a Comprehensive Treatise*; Franks, F., Ed.; Plenum Press: New York, 1972; Vol. 2, Chapter 5.

(8) Rowlinson, J. S.; Swinton, F. L. *Liquids and Liquid Mixtures*, 3rd ed.; Butterworths: London, 1982.

(9) Ben-Naim, A. *Water and Aqueous Solutions−Introduction to a Molecular Theory*; Plenum Press: London, 1975.

(10) Frank, H. S.; Evans, M. W. *J. Chem. Phys.* **1945**, *13*, 507.

(11) Strehlow, H.; Schneider, H. *Pure Appl. Chem.* **1971**, *25*, 327.

(12) Soper, A. K.; Finney, J. L. *Phys. Rev. Lett.* **1993**, *71*, 4346.

(13) Svishchev, I. M.; Kusalik, P. G. *J. Chem. Phys.* **1993**, *99*, 3049.

(14) Svishchev, I. M.; Kusalik, P. G. *Science* **1994**, *265*, 1219.

(15) Svishchev, I. M.; Kusalik, P. G. *J. Chem. Phys.* **1994**, *100*, 5165.

(16) Okazaki, S.; Nakanishi, K.; Touhara, H. *J. Chem. Phys*. **1983**, *78*, 454. Okazaki, S.; Touhara, H.; Nakanishi, K. *Ibid.* **1984**, *81*, 890.

(17) Bolis, G.; Corongiu, G.; Clementi, E. *Chem. Phys. Lett*. **1982**, *86*, 299.

(18) Jorgensen, W. L.; Madura, J. D. *J. Am. Chem. Soc*. **1983**, *105*, 1407.

(19) Stouten, P. F. W.; Kroon, J. *Mol. Simul.* **1990**, *5*, 175.

(20) Berendsen, H. J. C.; Postma, J. P. M.; van Gunsteren, W. F.; Hermans, J. *Intermolecular Forces*; Pullman, B., Ed.; Reidel: Dordrecht, 1981; p 331.

(21) Stouten, P. F. W.; Kroon, J. *J. Mol. Struct.* **1988**, *177*, 467.

(22) Ferrario, M.; Haughney, M.; McDonald, I. R.; Klein, M. L. *J. Chem. Phys.* **1990**, *93*, 5156.

(23) Palinkas, G.; Hawlicka, E.; Heinzinger, K. *Chem. Phys.* **1991**, *158*, 65.

(24) Palinkas, G.; Bako, I.; Heinzinger, K.; Bopp, P. *Mol. Phys*. **1991**, *73*, 897.

(25) Palinkas, G.; Bako, I. *Z. Naturforsch.* **1991**, *46a*, 95.

(26) Tanaka, H.; Walsh, J.; Gubbins, K. E. *Mol. Phys*. **1992**, *76*, 1221.

(27) Tanaka, H.; Gubbins, K. E. *J. Chem. Phys*. **1992**, *97*, 2626.

(28) Haughney, M.; Ferrario, M.; McDonald, I. R. *J. Phys. Chem*. **1987**, *91*, 4934.

(29) Allen, M. P.; Tildesley, D. J. *Computer Simulation of Liquids*; Oxford University Press: New York, 1987.

(30) Fincham, D. *CCP5 Q. Newslett*. **1981**, *2*, 6.

(31) Ewald, P. *Ann. Phys*. **1921**, *64*, 253.

(32) Brooks, C. L., III. *J. Chem. Phys*. **1987**, *86*, 5156.

(33) Laaksonen, A. *Comput. Phys. Commun.* **1986**, *42*, 271.

(34) Hoheisel, C. *Theoretical Treatment of Liquids and Liquid Mixtures*; Elsevier: New York, 1993.

(35) Palinkas, G.; Bopp, P.; Jancso, G.; Heinzinger, K. *Z. Naturforsch*. **1984**, *39a*, 79. Palinkas, G.; Hawlicka, E.; Heinzinger, K. *J. Phys. Chem*. **1987**, *91*, 4334.

(36) van Gunsteren, W. F.; Berendsen, H. J. C. *Mol. Phys*. **1977**, *34*, 1311.

(37) It is advisable to save the eigenvectors after diagonalization and use them as input in diagonalizing the moment of inertia tensor after the next time step. This will both speed up the diagonalization and keep the directions of the principal axes fixed.

(38) Liu, Q.; Brady, J. W. *J. Am. Chem. Soc*. **1996**, *118*, 12276.

(39) Micali, N.; Trusso, S.; Vasi, C.; Blaudez, D.; Mallamace, F. *Phys. Rev. E* **1996**, *54*, 1720.